Computing Quantum Bound States on Triply Punctured Two-Sphere Surface

K. T. Chan[1,2**], H. Zainuddin[1,2], K. A. M. Atan[2], A. A. Siddig[3]

[1]*Department of Physics, Faculty of Science, Universiti Putra Malaysia, UPM Serdang 43400, Malaysia*
[2]*Institute for Mathematical Research, Universiti Putra Malaysia, UPM Serdang 43400, Malaysia*
[3]*Department of Physics and Astronomy, College of Science, King Saud University, Riyadh 11451, Saudi Arabia*

(Received 17 March 2016)

We are interested in a quantum mechanical system on a triply punctured two-sphere surface with hyperbolic metric. The bound states on this system are described by the Maass cusp forms (MCFs) which are smooth square integrable eigenfunctions of the hyperbolic Laplacian. Their discrete eigenvalues and the MCF are not known analytically. We solve numerically using a modified Hejhal and Then algorithm, which is suitable to compute eigenvalues for a surface with more than one cusp. We report on the computational results of some lower-lying eigenvalues for the triply punctured surface as well as providing plots of the MCF using GridMathematica.

PACS: 03.65.Ge, 02.40.−k, 02.60.−x DOI: 10.1088/0256-307X/33/9/090301

In 1924, Emil described the geodesic motion of free particle on a non-compact Riemann surface, $\Gamma\backslash\mathcal{H}$, where $\mathcal{H}$ is the upper half plane, and Γ is the modular group.[1] Such non-compact Riemann surfaces of finite area have vertices that are located infinitely far away (i.e., cusps) and they can be used as mathematical models for many physical situations such as in the scattering problem where a particle enters and exits a cavity via the cusp. Of particular interest is the quantum version of such scattering problems.[2] Studies of classical and quantum billiards on hyperbolic surfaces have attracted wide attention of both mathematicians and physicists as these systems are connected to problems in number theory, differential geometry, group theory[3] as well as in quantum chaos.[4−6] Such systems can also be realized experimentally via hyperbolic optical and microwave cavities.[7−9]

In this Letter, we are interested in a triply punctured two-sphere surface (surface of genus zero and three cusps)[10] which is formed from the quotient of the upper half plane by a discrete subgroup of the modular group, that is, the principal congruence subgroup of level two. Since this hyperbolic surface is strongly chaotic, ergodic and with multiple cusps, it is therefore an interesting candidate for the study of chaotic scattering with multi-scattering channels.[11] It is also known that systems of particle on noncompact finite area hyperbolic surfaces exhibit both discrete and continuous spectra.[12] The scattering states are described by the Eisenstein series, which is known analytically,[13−15] while the bound states have to be computed numerically. For a triply punctured two-sphere surface, the bound states have not been explicitly calculated and thus are our main concern here.

In solving a bound state problem on a triply punctured two-sphere surface, we need to solve the Schrödinger equation $H\psi = E\psi$, where Hamiltonian $H = -\Delta$, and $\Delta = y^2(\partial_x^2 + \partial_y^2)$ is the Laplace-Beltrami operator ($\hbar = 2m = 1$), and E is discrete. The solution to this quantum system is known as the Maass cusp forms (MCFs).[13] There are special boundary conditions (automorphy condition) to be satisfied by MCFs, i.e., $\psi(z) = \psi(Tz) = \psi(z^*)$ for all $T \in \Gamma(2)$ and $z \in \mathcal{H}$. We report here on some computed low-lying eigenvalues using an adapted algorithm of Hejhal and Then.[16−18] Eigenvalues computed from this surface are then checked by using selected procedures such as the Hecke relation and the Ramanujan–Petersson conjecture for their authenticity. These eigenvalues are particularly useful for finding the renormalized time delay of the chaotic system. We later exploit the graphical capability of GridMathematica to visualize the eigenstates of selected eigenvalues.

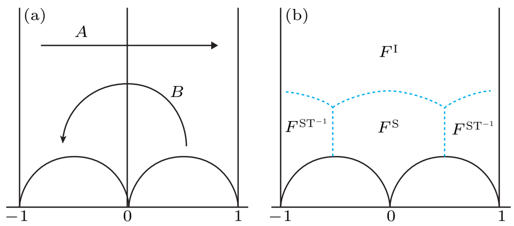

Fig. 1. (a) Fundamental domain of the principal congruence subgroup $\mathcal{F}_2$. (b) Subdomains of $\mathcal{F}_2$ subjected to $N_1 = I$.

Mathematically, the triply punctured two-sphere surface is represented by the fundamental domain of the principal congruence subgroup of level two, i.e., $\Gamma(2) = \begin{pmatrix} a & b \\ c & d \end{pmatrix} \in SL(2,\mathbb{Z})$ such that $b \equiv c \equiv 0 \bmod 2$ and $a \equiv d \equiv 1 \bmod 2$. The subgroup has two generators $A = \begin{pmatrix} 1 & 2 \\ 0 & 1 \end{pmatrix}$ and $B = \begin{pmatrix} 1 & 0 \\ -2 & 1 \end{pmatrix}$[10] and their Möbius transformation are given as $A : z \to z + 2$ and $B : z \to \frac{z}{-2z+1}$. Fundamental domain $\mathcal{F}_2$ for the punctured sphere[10,19] as shown in Fig. 1(a) is formed with

**Corresponding author. Email: chankt@upm.edu.my

side identifications by using transformations A and B. Through the identification process, we obtain a sphere with three inequivalent cusps, that is, the points at ∞, 0 and 1 where they are mathematically referred to as parabolic fixed points (the scattering channels). Parabolic transformations $\{A, B, B^{-1}A^{-1}\}$ are used to fix the cusps $\{\infty, 0, 1\}$, respectively.[18]

The fundamental domain is then partitioned into three subdomains (Fig. 1(b)), that is, $N_j\mathcal{F}^I$, $N_j\mathcal{F}^S$ and $N_j\mathcal{F}^{ST^{-1}}$ with respect to the inequivalent cusp classes. Here I refers to identity, $T : z \to z+1$ and $S : z \to -\frac{1}{z}$. The location of these subdomains can be changed to their equivalent ones when they are subjected to different cusp normalizing maps $N_j = \{I, S, ST^{-1}\}$, respectively.[18] This process is important due to the fact that the group-theoretic features of the fundamental domain enable us to simplify the MCF expansion as well as the pullback algorithm which is used to map evenly spaced points given as $z_k = x_k + iy = \frac{L}{2Q}(k-0.5) + iy \in \mathcal{H}$ for $1 \le k \le Q$ and $y < y_0$ into the fundamental domain from its exterior. The number $Q \in \mathbb{Z}$ is the total number of sampling points, and y_0 is the minimal height for the fundamental domain. For each j and k, pullback of $N_j^{-1}(z_k)$ is computed by applying a map $T_{kj} \in \Gamma(2)$ such that $w = T_{kj}N_j^{-1}(z_k) \in \mathcal{F}_2$. Hence, the complete pullback is given as

$$z^*_{kj} = x^*_{kj} + y^*_{kj} = N_{I(w)}U_w(w), \tag{1}$$

where $I(w)$ refers to indices $\{1,2,3\}$, and $U_w(w)$ is a map that maps vertex of $\mathcal{F}_2$ to its nearest inequivalent cusp. Location of each pullback point at different vertices inside the fundamental domain can be identified by using a point locater algorithm (details in Ref. [18]). Based on the complete pullback, some important pullback relations between points in each subdomain are

$$\mathcal{F}^I = S\mathcal{F}^S = ST^{-1}\mathcal{F}^{ST^{-1}}, \tag{2}$$
$$\mathcal{F}^S = S\mathcal{F}^I, \tag{3}$$
$$S\mathcal{F}^{ST^{-1}} = ST^{-1}\mathcal{F}^S. \tag{4}$$

The algorithm to compute MCF for this punctured surface is based on the adapted algorithm of Hejhal and Then,[16,17] but now expanded to several cusps. This modification is inspired by the algorithm created by Ref. [19] where they used Hejhal's algorithm on several cusps in the study of holomorphic cusp forms and also work from Ref. [20] for Hecke congruence subgroup. Since the surface has three cusps, the numerical method requires Fourier expansions at all cusps of $\mathcal{F}_2$ which is given as

$$\psi_j(x+iy) = \sum_{|n|\ge 1} a_j(n)k_n(y)e^{(\frac{2\pi inx}{L})}, \quad j \in \{1,2,3\}, \tag{5}$$

where $k_n(y) = y^{1/2}K_{ir}(\frac{2\pi ny}{L})$, j represents the inequivalent cusps, and K_{ir} is the K-Bessel function.[13] Truncating Eq. (5) and applying the reflection symmetry at the imaginary axis y, we obtain

$$\psi_j(z) = \sum_{n=1}^{M} a_j(n)k_n(y)\mathrm{cs}\Big(\frac{2\pi nx}{2}\Big) + [[\epsilon]], \tag{6}$$

where $\mathrm{cs}(\frac{2\pi nx}{2})$ represents either $2\sin(\frac{2\pi nx}{2})$ or $2\cos(\frac{2\pi nx}{2})$ for odd and even classes, respectively, while $M = M(r,y)$ is the truncating point, and $[[\epsilon]]$ represents the error term. To make the algorithm stable, we have to expand MCF at different subdomains ($\mathcal{F}^I$, $\mathcal{F}^S$ and $\mathcal{F}^{ST^{-1}}$). Taking the finite Fourier transform for Eq. (6) and applying the special boundary conditions, we obtain

$$a_j(m)k_m(y) = \frac{1}{2Q}\sum_{k=1}^{2Q}\psi_{I(j,k)}(z^*_{kj})\mathrm{cs}\Big(-\frac{2\pi mx_k}{2}\Big) + [[\epsilon]]. \tag{7}$$

As long as we choose $y < y_0$, we can use the truncation points $M_0 = M(y_0)$ for all series. With given values of r and y, we set the truncating points M_0 by using $M_0 = \frac{L(r+Dr^{1/3})}{2\pi y_0}$, where constant D is chosen among 8, 12 and 15[20,21] depending on the required accuracy. Hence we obtain the following relation for the Fourier coefficients

$$a_j(m)k_m(y) = \sum_{i=1}^{3}\sum_{n=1}^{M_0} a_i(n)V^{ji}_{mn} + 2[[\epsilon]], \tag{8}$$

where

$$V^{ji}_{mn} = \frac{1}{2Q}\sum_{k=1,I(j,k)=i}^{2Q} k_n(y^*_{kj}) \cdot \mathrm{cs}\Big(\frac{2\pi nx^*_{kj}}{2}\Big)\mathrm{cs}\Big(\frac{-2\pi mx_k}{2}\Big). \tag{9}$$

Note that $I(j,k) = i$ denotes that the summation is restricted to those values of k for which $I(w) = I(T_{kj}N_j^{-1}(z_{kj}))$. In other words, summation is carried out only to pullback points located on the particular i subdomains. By neglecting the error term $2[[\epsilon]]$ and taking pullback relations (Eqs. (2)–(4)) into consideration, we reduce Eq. (8) into a linear imhomogeneous equation for which the Fourier coefficients can be solved. To locate the eigenvalues, we compute g_m values defined as

$$g_m = \sum_{i=1}^{3}\sum_{n=1}^{M_0} a_i^{\#1}(n)\widetilde{V}^{ji}_{mn}(r, y_2), \tag{10}$$

where $y_2 = 0.9y_1$ is considered as a choice of independent y value,[13] while $a_i^{\#1}(n)$ are coefficients obtained by solving Eq. (8). We look for simultaneous changes of sign in g_m to determine the candidate interval for the eigenvalues.

The computational work in this study is based on an existing GridMathematica program for the modular group[17] which is now modified for the sphere with three cusps. Writing $E = 1/4 + r^2$, we compute eigenvalues for the triply punctured two-sphere surface for the r-interval[1,14] on a quad core processor CPU of 3.07 GHz and 4 GB of memory. In this interval, we found 20 eigenvalues of which 11 belong to the odd class and nine to the even class as shown in Table 1. We have set the tolerance to be $\epsilon = 10^{-6}$ in our bisection module and as such our eigenvalues are estimated to be accurate at least up to five decimal places. The smallest true eigenvalue is $E = 13.96448866$ with $r = 3.7033078$, which belongs to the odd class. For the even class, the smallest true eigenvalue is $E = 34.81680463$ with $r = 5.8793541$. A mixture of eigenvalues belonging to eigenfunctions of the modular group, i.e., oldforms (eigenvalue with an asterisk in Table 1) and new ones directly corresponding to $\varGamma(2)$, i.e., newforms can be seen from the computed eigenvalues for both classes. The appearance of both oldforms and newforms is a positive indication that our computation is correct.

To check on the authenticity of the eigenvalues, we need to compute the Fourier coefficients for the odd and even MCFs for all Hecke operators T_n with $\gcd(n, 2) = 1$. One can show that $T_n\psi(z) = t_n\psi(z)$, which means that the eigenvalue of any wave function for the nth Hecke operator is the nth Fourier coefficients of the expansion of $\psi(z)$. Tables 2 and 3 list some of the Fourier coefficients for selected odd and even classes' eigenvalues. Such arithmetic structures are expected,[3] since principal congruence subgroup and the modular group are arithmetic groups. In Ref. [22], it is mentioned that for any arithmetic group or subgroup, all Fourier coefficients must satisfy the Ramanujan–Petersson conjecture i.e., $|a_p| < 2$ for all primes p. Based on the results from Tables 2 and 3, all the prime coefficients from both classes agree well with the conjecture, which further support the authenticity of the eigenvalues.

Other supporting evidence is the use of the Hecke relation, i.e., multiplicative relation for the Fourier coefficients, $a_{mp} = a_m a_p - a_{\frac{m}{p}}$, where p is a prime with the convention $a_{\frac{m}{p}} = 0$ if p does not divide m. This method is only applicable to the arithmetic group (or its subgroups).[22] As an example, we use $r = 6.6204223$ and $r = 10.9203917$ from the odd and even classes respectively to check on their coefficients' multiplicative relation. From Table 3, we can see that coefficients a_{15} and a_{21} agree with the multiplicative relation. The value on the left-hand side coincides with the right-hand side up to a minimum of four decimal places.

Table 1. The eigenvalues of the Laplacian for the triply punctured two-sphere surface. Listed are odd and even r-values related to the true eigenvalues via $E = \frac{1}{4} + r^2$.

Odd r-values		Even r-values	
3.7033078	9.5336951*	5.8793541	12.8776165
5.4173348	9.9349198	8.0424776	13.1720749
6.6204223	11.3176796	9.8598964	13.7797514*
7.2208719	11.9727767	10.9203917	
8.2736658	12.1730084*	11.4930046	
8.5225029		12.0929949	

Table 2. Fourier coefficients for selected eigenvalues of odd and even MCFs.

	Odd r-values		Even r-values	
a_n	7.2208719	9.5336951	11.4930046	13.7797514
a_1	1	1	1	1
a_3	−0.94935041	−0.456196732	0.177099498	0.246899572
a_5	−0.86971293	−0.290672326	−0.527814612	0.737060671
a_7	−0.061359596	−0.744941725	1.123057613	−0.261230404
a_9	−0.098733545	−0.791883223	−0.968637269	−0.939041371
a_{11}	−0.074141641	0.166163363	−1.015447918	−0.953563505
a_{13}	−0.086312577	−0.586688754	−1.807538347	0.278827573
a_{15}	0.825663215	0.132604065	−0.093469832	0.181979499
a_{17}	−1.694902025	0.57069581	−0.000328076	1.30734199
a_{19}	1.423495076	−0.98193619	−0.961584897	0.092558161
a_{21}	0.058252337	0.339840249	0.198893507	−0.064544679

Table 3. Fourier coefficients for 6.6204223 (odd r-value) and 10.9203917 (even r-value) together with their multiplication relation.

a_n	6.6204223	$a_m a_p$	10.9203917	$a_m a_p$
a_3	1.210255527		−1.401733778	
a_5	1.288538066		0.852892885	
a_7	−0.351110172		0.324097545	
a_9	0.464704585		0.96485517	
a_{11}	0.217644948		0.223766949	
a_{13}	−1.229192055		1.308385204	
a_{15}	1.559440896	1.559460316	−1.195526775	−1.195528766
a_{17}	−0.570260658		1.329613996	
a_{19}	−0.259181147		−0.404857209	
a_{21}	−0.424933716	−0.424933026	−0.454293413	−0.454298477

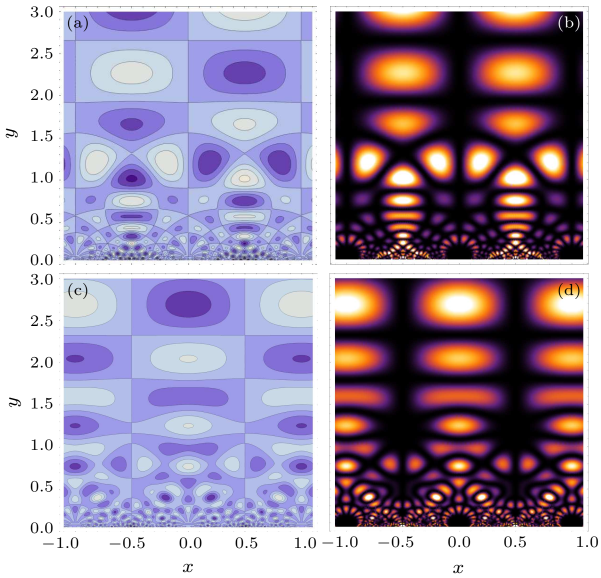

Fig. 2. (a)–(d) Eigenstates for odd eigenvalue $r = 12.1730084$ and even eigenvalue $r = 13.7797514$ in the form of contour plot and density plot, respectively. The illustrated region is $[-1.1, 1.1] \times [0.05, 3]$.

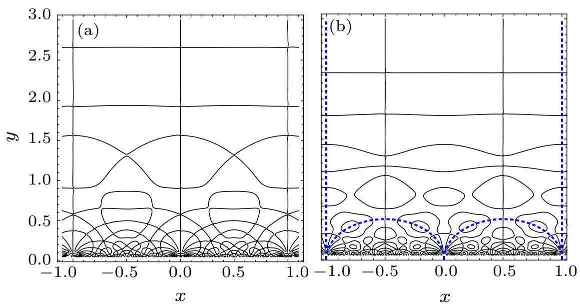

Fig. 3. (a)–(b) Nodal lines for odd ($r = 12.1730084$) and even ($r = 13.7797514$) eigenvalues, respectively. The illustrated regions are $[-1.1, 1.1] \times [0.05, 3]$.

Topography of the MCF on the triply punctured two-sphere surface are visualized by using contour plot and density plot functions of the GridMathematica. Figure 2 shows the topography of eigenstates for odd and even eigenvalues, $r = 12.1730084$ and $r = 13.7797514$, respectively. Based on Fig. 2, we manage to identify the minimum (dark colour) and maximum spots (bright color) as well as the nodal lines ($\psi = 0$) for the MCF for each eigenstates. Nodal lines for the odd and even classes are shown in Fig. 3. The blue dashed lines in Fig. 3(b) indicate the boundary of the fundamental domain. The density plots show the probability function associated to ψ (i.e. $|\psi|^2$). The bright (dark) regions in Figs. 2(b) and 2(d) actually show regions of higher (lower) probability of finding the particle associated to the corresponding MCF. As the eigenvalues increase, more and more bright spots appear implying that the quantum particle is less localized at higher energies. It is interesting to note that one can make comparisons between the present case of triply punctured two-sphere surface and the earlier work for a singly punctured two-torus surface[16] since they have the same fundamental domain (see Fig. 1(a)) but with different side identifications. Comparing the eigenvalues of both cases, one finds that the lowest bound eigenvalue is lower in the case of the singly punctured two-torus surface. In addition, the punctured torus has degenerate eigenvalues implying additional symmetries within the structure. It is still not particularly clear how the underlying geometry affects these eigenvalues.

In summary, we have successfully computed 20 low-lying eigenvalues for the triply punctured two-sphere surface using a modified Hejhal and Then algorithm for several cusps. Eigenvalues from both classes satisfy the Ramanujan–Petersson conjecture and also the Hecke relation and hence support their authenticity. These eigenvalues may find use in obtaining the renormalized time delay of the chaotic system as stated in Refs. [11,23]. With further computation of these eigenvalues, one can also study the spectral statistics indicating fingerprints of quantum chaos.[1] In addition to the eigenvalues, we have shown that the topography of the eigenstates can be visualized by using contour plot and density plot functions of the GridMathematica. This may further aid understanding of the underlying quantum chaotic system with multiple scattering channels.

References

[1] Bolte J et al 1992 *Phys. Rev. Lett.* **69** 2188
[2] Gutzwiller M C 1990 *Chaos in Classical and Quantum Mechanics* (New York: Springer-Verlag)
[3] Bogomolny E et al 1995 *Chaos Solitons Fractals* **5** 1311
[4] Then H 2007 arXiv:0712.4322[nlin.CD]
[5] Hurt N E 2000 *Mathematical Physics of Quantum Wires and Devices* (Dordrecht: Kluwer Academic Publishers)
[6] Gubin A and Santos L F 2012 *Am. J. Phys.* **80** 246
[7] Wirzba A 1999 *Phys. Rep.* **309** 1
[8] Gabrielse G et al 1990 *Quantum Electrodynamics* (Singapore: World Scientific Publishing) chap 9
[9] Ginis V et al 2012 *New J. Phys.* **14** 033007
[10] Stillwell J 1992 *Geometry of Surfaces* (New York: Springer-Verlag)
[11] Levay P 2000 *J. Phys.* A **33** 4357
[12] Borthwick D 2012 *Spect. Geometry* **84** 1
[13] Then H 2004 *Math. Comput.* **74** 363
[14] Terras A 1985 *Harmonic Analysis on Symmetric Spaces and Application* I (New York: Springer-Verlag)
[15] Kubota T 1973 *Elementary Theory of Eisenstein Series* (New York: Tokyo and Halsted Press)
[16] Chan K T et al 2013 *Chin. Phys. Lett.* **30** 010304
[17] Chan K T et al 2013 *Sains Malays.* **42** 655
[18] Chan K T et al 2014 *AIP Conf. Proc.* **1588** 230
[19] Selander B and Strömbergsson A 2002 *UUDM Report* (Sweden: Uppsala University)
[20] Strömberg 2005 *PhD Dissertation* (Sweden: Uppsala University)
[21] Hejhal D A and Rackner B N 1992 *Exp. Math.* **1** 275
[22] Farmer D and Lemurell S 2005 *Math. Comput.* **74** 1967
[23] Cunden F D et al 2016 *J. Phys.* A **49** 18LT01